Fluorescent Probes of the Orientation of Myosin Regulatory Light Chains in Relaxed, Rigor, and Contracting Muscle

Nicholas Ling,* Carolyn Shrimpton,‡ John Sleep,‡ John Kendrick-Jones,§ and Malcolm Irving‡
*Department of Biological Science, The University of Waikato, Hamilton, New Zealand; ‡The Randall Institute, King's College London, London WC2B 5RL, England; and §MRC Laboratory of Molecular Biology, Cambridge CB2 2QH, England

ABSTRACT The orientation of the light-chain region of myosin heads in relaxed, rigor, and isometrically contracting fibers from rabbit psoas muscle was studied by fluorescence polarization. Cysteine 108 of chicken gizzard myosin regulatory light chain (cgRLC) was covalently modified with iodoacetamidotetramethylrhodamine (iodo-ATR). Native RLC of single glycerinated muscle fibers was exchanged for labeled cgRLC in a low [Mg^{2+}] rigor solution at 30°C. Troponin and troponin C removed in this procedure were replaced. RLC exchange had little effect on active force production. X-ray diffraction showed normal structure in rigor after RLC exchange, but loss of axial and helical order in relaxation. In isolated myofibrils labeled cgRLC was confined to the regions of the sarcomere containing myosin heads. The ATR dipoles showed a preference for orientations perpendicular to the fiber axis, combined with limited nanosecond rotational motion, in all conditions studied. The perpendicular orientation preference was more marked in rigor than in either relaxation or active contraction. Stretching relaxed fibers to sarcomere length 4 μm to eliminate overlap between actin- and myosin-containing filaments had little effect on the orientation preference. There was no change in orientation preference when fibers were put into rigor at sarcomere length 4.0 μm. Qualitatively similar results were obtained with ATR-labeled rabbit skeletal RLC.

INTRODUCTION

Filament sliding and force production in muscle are generally assumed to be driven by a conformational change or working stroke in the globular head region of myosin while it is bound to actin during the cyclical interaction between the two proteins and ATP (A. F. Huxley, 1957; Reedy et al., 1965; H. E. Huxley, 1969; Lymn and Taylor, 1971; A. F. Huxley and Simmons, 1971; Rayment et al., 1993a). Such a working stroke would necessarily involve a change in the orientation of all or part of the myosin head with respect to the fiber axis. This can be investigated by attaching a fluorescent, phosphorescent, or spin probe to a specific site on the head and measuring the orientation of the probe dipole with respect to the direction of an applied electromagnetic field. Such probes have usually been attached to the most reactive thiol, SH1 or Cys 707, of the myosin heavy chain (Thomas and Cooke, 1980; Borejdo et al., 1979, 1982; Cooke et al., 1982; Tanner et al., 1992; Ostap et al., 1995). The active site of the myosin head has also been probed with nucleotide analogs (Yanagida, 1981; Crowder and Cooke, 1987). These studies have demonstrated a high degree of order of dipole orientations in the absence of ATP (the rigor state, which is usually considered to correspond to the structure at the end of the working stroke). However, in both relaxed and actively contracting muscle the dipole orientations were disordered, and most studies have failed to detect any oriented population of dipoles distinct from that in rigor. Acetamidotetramethylrhodamine (ATR) probes on Cys 707 do show large differences in orientation between contraction and rigor (Burghardt et al., 1983), but this probe may report a local structural change associated with nucleotide binding rather than a global change in head conformation associated with force generation (Tanner et al., 1992). This probe does not change orientation during the rapid force recovery that follows a submillisecond shortening step (Berger et al., 1994).

These negative results suggest that most of the catalytic domain of the myosin head, containing Cys 707 and the actin-binding and active sites, does not undergo a large-scale orientation change during force generation. However, they do not exclude models for the working stroke involving internal bending of the head, in which only the light-chain region, farthest from actin, undergoes a large change in orientation (Cooke, 1986; Thomas, 1987; Vibert and Cohen, 1988). Such models are consistent with the crystal structure of the myosin head (Rayment et al., 1993b), which shows that the light-chain region could act as a lever arm, converting relatively small-scale structural changes in the catalytic domain to movements of several nanometers at the head-rod junction.

This type of model for the working stroke can be tested with probes on the light-chain domain. The regulatory light chain (RLC) is readily removed from permeabilized muscle fibers (Moss et al., 1982) and can be replaced by RLC that has been covalently modified with a suitable probe molecule (Irving et al., 1989; Hambly et al., 1991, 1992). We used this approach to introduce ATR-labeled RLC into glycerinated rabbit psoas fibers and measured dipole orientations by steady-state fluorescence polarization. For most of the experiments we used chicken gizzard RLC because it contains only one thiol group (Cys 108), and therefore

Received for publication 12 September 1995 and in final form 10 January 1996.

Address reprint requests to Dr. Malcolm Irving, The Randall Institute, King's College London, 26-29 Drury Lane, London WC2B 5RL, England.

0006-3495/96/04/1836/11 $2.00

specific labeling is easily achieved. The main experiments were repeated with rabbit skeletal RLC, which has two thiols (Cys 127 and Cys 156; Matsuda et al., 1977). This paper describes the experimental approach and some of its limitations, and its application to steady-state orientations of the RLC probes in relaxation, rigor, and isometric contraction. An accompanying paper (Allen et al., 1996) describes time-resolved measurements of the changes in orientation of the same light-chain probe accompanying initiation of active contraction or relaxation induced by photolysis of caged ATP. The orientation changes of the RLC probes produced by submillisecond-length steps have been described elsewhere (Irving et al., 1995).

MATERIALS AND METHODS

Preparation of ATR-labeled regulatory light chains

Chicken gizzard myosin regulatory light chain (cgRLC) was either isolated from gizzard as described by Jakes et al. (1976) or, in later experiments, expressed in *Escherichia coli* (Rowe and Kendrick-Jones, 1992). No differences were observed between the results obtained from these two cgRLC preparations. The single cysteine residue (Cys108) of cgRLC was covalently modified with iodoacetamidotetramethylrhodamine (iodo-ATR) (lot 9B or 10A; Molecular Probes, Eugene, OR) as follows: cgRLC (1 mg/ml) in storage solution (2 M urea, 100 mM NaCl, 1 mM $MgCl_2$, 0.2 mM dithiothreitol (DTT), 25 mM Tris-HCl, pH 7.5) was exchanged into 6 M guanidine hydrochloride (GnHCl), 20 mM DTT by centrifuging through a 1-ml minicolumn (Penefsky, 1977) of Sephadex G-50 (Pharmacia) equilibrated with this solution, and left for 1 h at room temperature to ensure complete reduction of thiol groups. It was then passed through another G-50 minicolumn equilibrated with labeling buffer (100 mM potassium propionate (KPr), 20 mM sodium phosphate (NaP_i), pH 6.5). Iodo-ATR from a stock solution (20 mM in dimethylformamide) was added to 200 μM final concentration, and labeling proceeded at room temperature in the dark for 36 h. Labeling was terminated by the addition of 2 mM DTT, and unbound iodo-ATR was removed by centrifuging through G-50 minicolumns equilibrated with extract solution (50 mM KPr, 20 mM EDTA, 10 mM potassium phosphate (KP_i), 0.5 mM DTT, pH 7.0). The final concentration of labeled RLC in extract solution was approximately 0.5 mg/ml.

Rabbit skeletal muscle RLC (rsRLC) was prepared from the back and leg muscles of male Dutch rabbits by DTNB (5,5′-dithio-bis-2-nitrobenzoic acid) isolation (Wagner, 1982) and labeled using the protocol described above for cgRLC. rsRLC has two cysteine residues at positions 127 and 156. The former is likely to be more reactive toward iodoacetamido-derivatives (Katoh and Lowey, 1989), but both thiols may be labeled to some extent in the present protocol.

Stoichiometry of labeling for ATR-conjugated RLC was estimated by measuring concentrations of ATR, assuming an extinction coefficient of 97,000 M^{-1} cm^{-1} at 549 nm as measured for the 5′ isomer of ATR (Corrie and Craik, 1994), and of RLC, using the bicinchoninic acid (BCA) assay (Pierce, Oud-Beijerland, The Netherlands). For chicken gizzard RLC the estimated stoichiometry was 0.36 ± 0.06 (mean ± SEM for six labeled batches); for rabbit skeletal RLC it was 0.46 ± 0.09 (n = 2).

Preparation of myosin subfragment-1 containing ATR-labeled RLC

Mg-papain subfragment 1 (S-1) was prepared by the method of Margossian and Lowey (1982). An aliquot of 10 mg/ml S-1 in extract solution was mixed with an equal volume of 1 mg/ml ATR-labeled cgRLC in extract solution and incubated in the dark at 30°C for 30 min. The proteins were then exchanged into 5 mM $MgCl_2$, 60 mM NaP_i, pH 6.0, using a centrifuge column as described above. Labeled RLC not bound to S-1 was removed by the addition of 1/10 volume of DE52 resin (Whatman), to which it bound, leaving the S-1 in solution. After centrifugation to pellet the DE52, the supernatant was dialyzed against rigor solution (130 mM KPr, 2.2 mM magnesium acetate (MgAc), 2.5 mM dipotassium ethyleneglycol-bis-(aminoethylether)-tetra-acetic acid (K_2EGTA), 10 mM imidazole, ionic strength 150 mM, pH 7.0).

Preparation of fibers for RLC exchange

Single fibers were dissected from glycerinated rabbit psoas muscle fiber bundles prepared as described by Peckham and Irving (1989). Fiber segments 2–4 mm in length had aluminium T-clips crimped to both ends and were transferred to a 40-μl glass trough on a temperature-controlled (10°C) microscope stage containing relaxing solution (80 mM KPr, 7 mM MgAc, 5 mM K_2EGTA, 5 mM Na_2ATP, 5 mM phosphocreatine (PCr), 25 mM imidazole, ionic strength 159 mM, pH 7.0, at 10°C). The fibers were suspended between two hooks, one of which was attached to a force transducer (AE801; Aksjeselskapet Mikro-elektronikk, Horten, Norway). The stage held five 40-μl glass troughs that could be rotated to change the solution bathing the fiber (Sleep, 1990). Sarcomere length and fiber diameter were measured using a 32× objective (Leitz L32, N.A. 0.40) and ocular micrometer, and hook separation was adjusted to set sarcomere length to 2.4 μm. The copper microscope stage was cooled by cold nitrogen gas or warmed by a closely opposed quartz halogen lamp. Trough temperature was controlled to ±0.1°C by varying the flow of cold nitrogen gas or the lamp current. Fibers were activated by transfer to a trough of preactivating solution (7 mM MgAc, 5 mM Na_2ATP, 0.2 mM K_2EGTA, 5 mM PCr, 25 mM imidazole, 90 mM KPr, ionic strength 155 mM, pH 7.0) followed by activating solution (40 mM KPr, 7 mM MgAc, 10 mM CaEGTA, 5 mM Na_2ATP, 10 mM PCr, 25 mM imidazole, ionic strength 150 mM, pH 7.0) for measurement of isometric force production at 10°C. Fibers were then returned to relaxing solution before RLC exchange.

Exchange of ATR-labeled RLC into muscle fibers

Preliminary experiments used the protocol of Moss et al. (1982), which involves removal of native RLC in an EDTA rigor extraction solution for 2 h at 30°C followed by incubation in exogenous RLC in relaxing solution. We subsequently found that the same degree of RLC exchange could be achieved with the briefer protocol described below, and this protocol was used for all of the experiments presented in the Results.

After isometric force measurement as above, the fiber was put into rigor in extract solution (50 mM KPr, 20 mM EDTA, 10 mM KP_i, 0.5 mM DTT, pH 7.0) at 10°C and then transferred to a solution of labeled RLC (approximately 0.5 mg/ml in extract solution), and the temperature was raised to 30°C for 30 min. The temperature was reduced to 10°C, and the fiber was washed briefly in relaxing solution, then incubated in troponin (0.5 mg/ml in relaxing solution, 10°C, 40 min) and troponin-C (0.5 mg/ml in relaxing solution, 10°C, 5 min) to replace these proteins removed during the RLC exchange step. Rabbit skeletal muscle troponin was purchased from Sigma; troponin C was prepared by the method of Greaser and Gergely (1971). The fiber was activated as before, and the isometric force was compared to the pre-exchange value.

Binding of myosin subfragment-1 to muscle fibers

Single glycerinated psoas fibers were mechanically skinned with electrolytically sharpened tungsten needles to facilitate entry of myosin S-1 (Peckham and Irving, 1989) and mounted on the microscope stage in relaxing solution as described above. The fiber was slowly stretched to a sarcomere length of 4.0 μm to eliminate overlap between actin- and myosin-containing filaments, then rinsed in rigor solution for 1 min. It was then transferred to rigor solution containing labeled S-1 (approximately 5

mg/ml) for 30 min at 10°C. The fiber was washed several times in rigor solution before fluorescence polarization measurements.

Fluorescence polarization measurements

Steady-state fluorescence polarization measurements on single muscle fibers were made using a modified Zeiss ACM microscope with epifluorescence condenser IV Fl. Light from a HBO 100-W mercury lamp was passed through a 540-nm, 30-nm FWHM interference filter, polarized by a rotatable polarizing prism, and reflected by the 580-nm dichroic mirror/filter assembly (Zeiss filter set 487714) through a 32× objective lens (Leitz 32×, N.A. 0.40) to illuminate the fiber with light polarized either parallel or perpendicular to the longitudinal fiber axis. A circular field aperture was focused to a 48-μm-diameter spot at the fiber. Fluorescent light was collected by the same objective lens and passed up the microscope axis through the dichroic mirror/filter assembly (barrier filter 590 nm, longpass). A circular aperture in the primary image plane coincided with the image of the spot on the fiber. A Wollaston beam-splitting prism separated the fluorescent light into components polarized parallel and perpendicular to the fiber axis, and the intensities of these components were measured with two photomultipliers.

Four fluorescence intensities were measured: ${}_{\parallel}I'_{\parallel}$, ${}_{\parallel}I'_{\perp}$, ${}_{\perp}I'_{\parallel}$, and ${}_{\perp}I'_{\perp}$, where ${}_{m}I'_{n}$ denotes the observed fluorescence intensity for exciting light of polarization m and fluorescent light of polarization n, and $\parallel$ and $\perp$ refer to linear polarizations parallel and perpendicular to the fiber axis. The observed intensities (${}_{m}I'_{n}$) depend on incident light intensity, photomultiplier gains, and the transmittances for parallel and perpendicular polarized light in the excitation and collection optics, as well as on the ideal intensities (${}_{m}I_{n}$) that would be measured at the fiber if the intensity of the exciting light were the same for the two polarizations. The relative instrumental gain factors (or parallel:perpendicular transmittance ratios) for the exciting and fluorescent light (including lamp polarization in the former case and photomultiplier gains in the latter) were obtained on each experimental day by measuring polarized intensities from a thin-walled glass capillary (50–100 μm diameter) or a 100-μm path-length microslide (Camlab, Cambridge, England) containing ATR-labeled RLC in solution, set up on the microscope stage in place of a fiber. These calculations assume an isotropic distribution of ATR in the capillary; this was checked by rotating the capillary through 90° on the microscope stage. Fluorescence intensities from the capillary were also used to obtain isotropic polarization ratios from ATR-labeled RLC in solution and to estimate the extent of RLC exchange in the fiber (see below). Background fluorescence intensity (no sample present) was subtracted from all sample measurements. In the case of fibers, the small autofluorescence intensity was measured from the unlabeled fiber before RLC exchange and subtracted.

After correction for background intensity and instrumental gain factors the polarized fluorescence intensities due to the fiber (${}_{m}I_{n}$) were used to calculate the conventional fluorescence polarization ratios:

$$P_{\parallel} = ({}_{\parallel}I_{\parallel} - {}_{\parallel}I_{\perp})/({}_{\parallel}I_{\parallel} + {}_{\parallel}I_{\perp}) \quad (1)$$

$$P_{\perp} = ({}_{\perp}I_{\perp} - {}_{\perp}I_{\parallel})/({}_{\perp}I_{\perp} + {}_{\perp}I_{\parallel}) \quad (2)$$

$$Q_{\parallel} = ({}_{\parallel}I_{\parallel} - {}_{\perp}I_{\parallel})/({}_{\parallel}I_{\parallel} + {}_{\perp}I_{\parallel}) \quad (3)$$

$$Q_{\perp} = ({}_{\perp}I_{\perp} - {}_{\parallel}I_{\perp})/({}_{\perp}I_{\perp} + {}_{\parallel}I_{\perp}). \quad (4)$$

The extent of RLC exchange in a fiber was estimated by comparing the fluorescence intensity of the relaxed fiber with that of a glass capillary containing a known concentration of ATR-labeled RLC in extract solution. For this purpose native RLC concentration in fibers was assumed to be 200 μM, and total fluorescence intensity was approximated by the expression ${}_{\parallel}I_{\parallel} + 2{}_{\parallel}I_{\perp} + 2{}_{\perp}I_{\parallel} + 8{}_{\perp}I_{\perp}/3$. This quantity is independent of dipole orientation for an immobile helical array of dipoles and can be shown, using the formalism of Irving (1996) and the orientation distributions described below, to give a good approximation to total fluorescence intensity for the largely disordered and partly mobile array of ATR dipoles present in relaxed muscle fibers. The cross-sectional areas of capillary or fiber illuminated were estimated as $2r^2(\alpha + \sin\alpha\cos\alpha)$ where $\sin\alpha = a/r$ and r = fiber or capillary radius, a = radius of illuminating spot (24 μm, $\leq r$). Rabbit psoas fibers used in this study had a mean diameter of 72 ± 2 μm (mean ± SEM, n = 60). The percentage RLC exchange was estimated as 48 ± 5% (mean ± SEM, n = 27) for cgRLC; and 28 ± 8% (n = 6) for rsRLC. The extent of RLC exchange was found to increase with increasing concentration of RLC in exchange solution and with decreasing fiber diameter.

Measurements of fluorescence intensity were made at three positions along each fiber in each solution, after tension had stabilized in the case of rigor or activation. Typically, measurements were taken for each fiber at least twice in relaxing and rigor solution in the following order: relaxing, rigor, relaxing, rigor, relaxing. Measurements of polarization ratios were found not to vary significantly between initial and subsequent solution changes (see below, Table 1), and the values reported in the part of the Results section after Table 1 are means of all measurements in relaxing or rigor solution in each fiber. Measurements from isometrically contracting fibers were made in a single activation for those fibers tested. In some experiments photobleaching of labeled fibers was reduced by the addition of 5 mM ascorbic acid or 0.1% 2-mercaptoethanol, 10 mM glucose, 0.1 mg/ml glucose oxidase, 0.023 mg/ml catalase (Kishino and Yanagida, 1988); these agents had a negligible effect on measured polarization ratios.

Exchange of ATR-labeled RLC into myofibrils

Myofibrils were prepared from fresh rabbit psoas muscle by the method of Knight and Trinick (1982) and stored at 4°C in rigor solution. An aliquot of myofibrils was washed several times in ice-cold rigor solution, and RLC was then extracted by incubation in extract solution at 30°C for 15 min. The myofibril suspension was centrifuged, the supernatant discarded, and the myofibrils incubated in 0.5 mg/ml ATR-labeled cgRLC in extract solution for 15 min at 30°C. Myofibrils were again washed in ice-cold rigor solution, then incubated in 0.5 mg/ml troponin in rigor solution for 15 min and in 0.5 mg/ml troponin C in rigor solution for 5 min. After further washing in rigor solution the labeled myofibrils were examined and photographed using an Axiovert 35 fluorescence microscope with a 100× plan Neofluor objective (1.3 NA).

X-ray diffraction of RLC-exchanged fibers

Low-angle x-ray diffraction patterns were recorded at station 2.1 of the Synchrotron Radiation Source (SRS), Daresbury, England, using a monochromator-mirror camera and gas-filled two-dimensional detector (Towns-Andrews et al., 1989). Bundles of three to nine psoas fibers were mounted

TABLE 1 Polarization ratios in repeated transitions between relaxation and rigor

	Relaxed	Rigor	Relaxed	Rigor	Relaxed
$P_{\parallel}$	0.340 ± 0.004	0.257 ± 0.010	0.341 ± 0.004	0.263 ± 0.009	0.344 ± 0.005
$Q_{\parallel}$	0.358 ± 0.005	0.284 ± 0.009	0.363 ± 0.005	0.290 ± 0.010	0.364 ± 0.005
$P_{\perp}$	0.423 ± 0.005	0.454 ± 0.008	0.422 ± 0.005	0.458 ± 0.009	0.421 ± 0.005
$Q_{\perp}$	0.440 ± 0.004	0.477 ± 0.008	0.442 ± 0.004	0.481 ± 0.007	0.440 ± 0.004

ATR-labeled chicken gizzard RLC; mean ± SE (n = 23); sarcomere length, 2.4 μm.

in relaxing or rigor solution between closely spaced mica windows at 20°C. The specimen-to-detector distance was 3 m. The diffraction patterns were analyzed using the BSL and OTOKO suites of programs supplied by the SRS. ATR-labeled cgRLC was exchanged into the bundles by the same procedure used for single fibers, but the percentage of RLC exchanged was lower in the bundles. It was estimated as 36 ± 4% (mean ± SEM, n = 5) by fluorescence intensity measurements on the individual fibers dissected from the labeled bundles.

RESULTS

Polarization ratios in relaxed and rigor fibers

In relaxed fibers into which chicken gizzard RLC had been exchanged the initial values of $P_{\|}$ and $P_{\perp}$ at sarcomere length 2.4 μm were 0.340 ± 0.004 (mean ± SEM, n = 23) and 0.423 ± 0.005, respectively (Table 1). Because $P_{\perp}$ is larger than $P_{\|}$, the ATR emission dipoles do not have an isotropic orientation distribution under these conditions; they have a small preference for orientations perpendicular to the fiber axis. The values of both $P_{\|}$ and $P_{\perp}$ are smaller than the isotropic polarization ratio measured on the same set-up for iodo-ATR immobilized in epoxy resin (0.475) but larger than that for cgRLC in solution, (0.264 ± 0.008, n = 6 labeling batches; same batches used in the fiber measurements). If the absorption and emission dipoles of ATR were exactly parallel and completely immobile during the nanosecond fluorescence lifetime, the value of the isotropic polarization ratio is expected to be 0.5. The observed value for iodo-ATR immobilized in epoxy (0.475) may be slightly smaller than 0.5 because of a small angular offset between absorption and emission dipoles for ATR, incomplete immobilization of the iodo-ATR in the epoxy, or instrumental imperfections. Whatever the relative contributions of these factors, the comparison between the fiber values and that for iodo-ATR in epoxy suggests that ATR on cgRLC in relaxed muscle fibers may have limited mobility on the fluorescence time scale.

When fibers were put into rigor $P_{\|}$ decreased and $P_{\perp}$ increased; this change was repeatable and fully reversible on subsequent relaxation (Table 1). In rigor the perpendicular orientation preference of the ATR emission dipoles was more pronounced than in relaxation.

The greater difference between $P_{\|}$ and $P_{\perp}$ in rigor indicates either greater order of dipole orientations or a stronger preference for perpendicular orientations.

The Q ratios, which depend on the orientation of the ATR absorption dipoles (see Materials and Methods, and Irving, 1996), were similar to the corresponding P ratios (dependent on the orientation of the emission dipoles) in both relaxing and rigor conditions (Table 1). There was a small systematic difference of about 0.02 between the P and Q ratios, however, which may indicate either a small angle between absorption and emission dipoles or, more likely, a small instrumental error. Because the difference is small and the two polarization ratios give similar information about ATR orientations, we report only the P ratios in the remainder of the Results.

Qualitatively similar results were obtained with ATR-labeled rabbit skeletal RLC (rsRLC), the native RLC in these fibers. Table 2 shows mean values for both types of RLC in relaxing and rigor conditions. The values of $P_{\|}$ and $P_{\perp}$ for cgRLC in Table 2 are slightly different from those in Table 1, reflecting the inclusion of results from more fibers, and the variability between different batches of labeled RLC and muscle fiber preparations. Despite this variability it is clear that the differences between rigor and relaxed P ratios were smaller for rsRLC than for cgRLC. Furthermore, the difference between $P_{\|}$ and $P_{\perp}$ was smaller for rsRLC than cgRLC in both relaxing and rigor conditions (Table 2), indicating a less pronounced preference for perpendicular orientations. The isotropic polarization ratio for rsRLC in solution, 0.248 ± 0.001 (two labeling batches), was slightly smaller than the value for cgRLC, 0.264 ± 0.008. rsRLC has two cysteine residues (127 and 156), and although residue 127 is expected to be more reactive with iodoacetamido derivatives (Katoh and Lowey, 1989), both residues may be labeled to some extent in our experiments. This may be responsible for the less marked orientation preference of the ATR dipoles with rsRLC than with cgRLC, which has a single cysteine at position 108. However, the different probe location or differences in structure of the two light chains or their interaction with the myosin heavy chain may also contribute to the observed difference in P ratios.

Effect of sarcomere length on polarization ratios in relaxed and rigor fibers

The orientation change seen on putting relaxed fibers into rigor is abolished by pre-stretching relaxed fibers to sarcomere length 4.0 μm to eliminate overlap between myofilaments (Table 3). A small decrease in $P_{\perp}$ accompanied the pre-stretch from sarcomere length 2.4 μm to 4.0 μm in relaxed fibers, and this was significant at the 5% level in paired comparisons. Little further change in $P_{\|}$ and $P_{\perp}$ occurred when the fibers were put into rigor at sarcomere length 4.0 μm, and neither of the rigor-relaxed paired differences at this sarcomere length were significant at the 5% level. The orientation distribution of ATR dipoles in both rigor and relaxing solution at sarcomere length 4.0 μm is similar to that in relaxing solution at sarcomere length 2.4

TABLE 2 Polarization ratios for chicken gizzard and rabbit skeletal RLC in relaxation and rigor

	$P_{\|}$	$P_{\perp}$
cgRLC relaxed	0.343 ± 0.003	0.432 ± 0.004
cgRLC rigor	0.242 ± 0.007	0.481 ± 0.005
cgRLC (rigor-relaxed)	−0.101 ± 0.008	0.049 ± 0.005
rsRLC relaxed	0.322 ± 0.003	0.396 ± 0.003
rsRLC rigor	0.281 ± 0.007	0.427 ± 0.004
rsRLC (rigor-relaxed)	−0.041 ± 0.004	0.031 ± 0.002

Mean ± SE (n = 39) for chicken gizzard RLC (cgRLC); n = 6 for rabbit skeletal RLC (rsRLC); sarcomere length, 2.4 μm.

TABLE 3 Effect of sarcomere length on polarization ratios in relaxation and rigor

	Sarcomere length (μm)	$P_{\parallel}$	$P_{\perp}$
Relaxed	2.4	0.361 ± 0.007	0.419 ± 0.010
Rigor	2.4	0.253 ± 0.011	0.472 ± 0.006
Rigor-relaxed	2.4	−0.108 ± 0.014	0.053 ± 0.008
Relaxed	4.0	0.355 ± 0.008	0.397 ± 0.009
Rigor	4.0	0.355 ± 0.013	0.408 ± 0.013
Rigor-relaxed	4.0	0.000 ± 0.006	0.011 ± 0.004

Mean ± SE (n = 5). Chicken gizzard RLC.

μm, and clearly different from that in rigor at 2.4 μm. The orientation change seen on putting relaxed fibers into rigor at the shorter sarcomere length is therefore likely to be due to binding of myosin heads to actin filaments.

Polarization ratios from ATR-labeled exogenous myosin subfragment 1 in rigor fibers

ATR-labeled chicken gizzard RLC was exchanged into isolated myosin S-1, which was then allowed to bind to rigor fibers at sarcomere length 4.0 μm. The resulting values of $P_{\parallel}$ and $P_{\perp}$ were 0.246 ± 0.004 (mean ± SEM, n = 6) and 0.504 ± 0.004, respectively. These values are similar but not identical to those obtained in rigor at short sarcomere length after exchanging the same light chain into native myosin heads, 0.242 ± 0.007 and 0.481 ± 0.005 (Table 2). This similarity supports the conclusion of the previous section that the orientation distribution of the probes on the light-chain region of the myosin heads in rigor is determined by binding of the heads to actin. It further suggests that the normal interaction between the myosin heads and the thick filament has only a small effect on the orientation distribution of this part of the myosin head under rigor conditions.

Temperature dependence of polarization ratios in relaxed fibers

X-ray diffraction studies have shown that the helical order of myosin filaments in relaxed rabbit psoas muscle fibers increases markedly with temperature in the range 5–20°C (Wray, 1987; Lowy et al., 1991), indicating greater alignment of the myosin heads along helical tracks on the surface of the thick filaments. However, the polarization ratios from ATR-labeled cgRLC in relaxed fibers showed very little dependence on temperature in this range. $P_{\parallel}$ was 0.354 ± 0.005 at 5°C, 0.349 ± 0.006 at 10°C, and 0.350 ± 0.003 at 20°C (means ± SE, n = 5). The corresponding values for $P_{\perp}$ were 0.432 ± 0.008, 0.430 ± 0.007, and 0.416 ± 0.007. The difference between the $P_{\perp}$ values at 5 and 20°C was significant at the 1% level in paired comparisons, but the absence of larger changes in the P ratios indicates that the present technique is relatively insensitive to the changes in helical order seen in the x-ray studies.

Isometric contraction

Isometric tension was hardly affected by the RLC exchange protocol. Tension after exchange of cgRLC was 93 ± 2% (n = 7) of the pre-exchange tension, and the corresponding value for rsRLC exchange was 91 ± 4% (n = 7). Polarization ratios in isometrically contracting fibers were similar to those during relaxation (Table 4) and clearly different from those in rigor (Table 1). The paired differences (contracting-relaxed) show a small but repeatable decrease in $P_{\perp}$ on activation for both cgRLC and rsRLC (Table 4). This small difference is in the direction opposite that of the change seen when relaxed fibers are put into rigor. Its origin is not clear, and a small effect of the opposite sign (i.e., toward the rigor value) is apparent in the comparison of the Q ratios after photolysis of caged ATP in the presence and absence of Ca^{2+} at 20°C (table 3 of Allen et al., 1996). Thus at present no clear effect on the polarization ratios can be attributed to active contraction per se. The distribution of RLC probe orientations is essentially the same during isometric contraction and relaxation. In both conditions there is likely to be a high degree of disorder of dipole orientations, which may be accompanied by restricted mobility of the dipoles on the nanosecond time scale.

X-ray diffraction of RLC-exchanged fibers

X-ray diffraction studies of small bundles of psoas fibers into which ATR-labeled cgRLC had been exchanged were carried out to see if RLC exchange altered the native filament structure. In relaxed fibers the equatorial intensity distribution, which is sensitive to the positions of the myosin heads in the plane perpendicular to the filament axis, showed a strong inner (1,0) equatorial reflection and weaker outer (1,1) reflection, both before and after exchange (Fig. 1 *A*, 20°C). The ratio of the intensities of the (1,1) and (1,0) reflections, $I(1,1)/I(1,0)$, was 0.32 in control bundles (Fig. 1, *continuous line*) and 0.40 after exchange (*dotted line*). The reflections shifted toward the center of the pattern after RLC

TABLE 4 Polarization ratios in relaxed and isometrically contracting fibers

	$P_{\parallel}$	$P_{\perp}$
cgRLC relaxed	0.342 ± 0.004	0.435 ± 0.006
cgRLC contracting	0.340 ± 0.005	0.421 ± 0.007
cgRLC (contracting-relaxed)	−0.002 ± 0.003	−0.014 ± 0.003
rsRLC relaxed	0.322 ± 0.003	0.396 ± 0.003
rsRLC contracting	0.321 ± 0.004	0.380 ± 0.003
rsRLC (contracting-relaxed)	−0.001 ± 0.003	−0.016 ± 0.001

Mean ± SE; n = 20 for chicken gizzard RLC; n = 6 for rabbit skeletal RLC; sarcomere length, 2.4 μm 10°C.

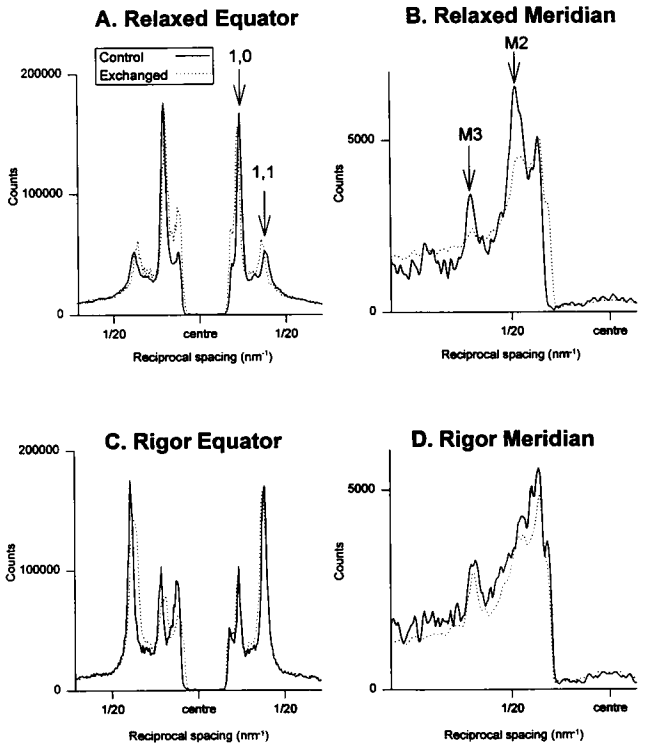

FIGURE 1 X-ray diffraction patterns from small bundles of psoas fibers before (control, *continuous lines*) and after RLC exchange (exchanged, *dotted lines*). (*A* and *C*) Equatorial intensity distribution in relaxing and rigor solutions, respectively, obtained by integrating the two-dimensional data from $\pm 1/100$ nm^{-1} on either side of the equator. (*B* and *D*) Meridional intensity distribution in relaxing and rigor solutions, respectively, obtained by integrating from $\pm 1/115$ nm^{-1} on either side of the meridian. The camera background, recorded with no fibers present, has been subtracted from the original two-dimensional data. (*A* and *B*) Control data, total of 72-s exposure from four bundles; exchanged data, 27-s exposure from five bundles. (*C* and *D*) Control data, 5-s exposure from one bundle; exchanged data, 70-s exposure from five bundles. The counts on the ordinate refer to rigor exchanged data. Data for other conditions were normalized to allow for variations in bundle size, beam intensity, and exposure time by scaling the two-dimensional patterns in the outer equator, from reciprocal spacing 1/21.4 to 1/13.3 nm^{-1}. Temperature 20°C.

exchange, showing that the filament lattice had swollen by about 5%. In rigor the (1,1) reflection was much stronger than the (1,0) in both exchanged and control fibers (Fig. 1 *C*); $I(1,1)/I(1,0)$ was 3.53 in control bundles and 3.75 after exchange. The rigor lattice was also swollen after RLC exchange, by about 3%. The equatorial reflection intensity changes shown in Fig. 1, *A* and *C* indicate that, both before and after RLC exchange, myosin heads were in the vicinity of the thick filaments and presumably detached from actin in relaxing conditions, and in the vicinity of the actin filaments and presumably attached to actin in rigor.

The meridional part of the x-ray diagram from control relaxed fibers (Fig. 1 *B*, *continuous line*) shows strong reflections from the axial periodicities of the thick filaments, at spacings of 21.5 nm (second-order myosin reflection, M2) and 14.3 nm (third-order myosin reflection, M3). These were much weaker after RLC exchange (Fig. 1 *B*, *dotted line*); the intensity of the 14.3-nm reflection was only about 23% of that in the control fibers. A similar reduction of intensity was observed for the myosin layer lines, which result from the helical order of the myosin heads; after exchange the intensity of the first myosin layer line, with a spacing of 43 nm, was about 35% of the control value (not shown). Thus either the exchange protocol or the presence of the labeled exogenous light chain disrupts the normal axial and helical order of relaxed fibers.

In contrast, RLC exchange had little effect on either meridional or layer line intensities in rigor. The intensity of the M3 meridional reflection at 14.5 nm after RLC exchange was 94% of the control value (Fig. 1 *D*). The first actin layer line at a spacing of 37 nm also remained strong (not shown).

Location of ATR-labeled RLC in myofibrils

Fluorescence micrographs of myofibrils containing ATR-labeled cgRLC showed that the exogenous RLC is confined to the A bands of the sarcomere (Fig. 2). Moreover, there was a dark band in the middle of each A band (*arrows*) corresponding to the position of the M-line or bare zone of the thick filaments where there are no myosin heads. These results are consistent with specific exchange of ATR-labeled RLC into the myosin heads.

DISCUSSION

Limitations of the ATR-RLC probe

An ideal extrinsic orientation probe would satisfy two key criteria: accurate reporting of the orientation of a specific

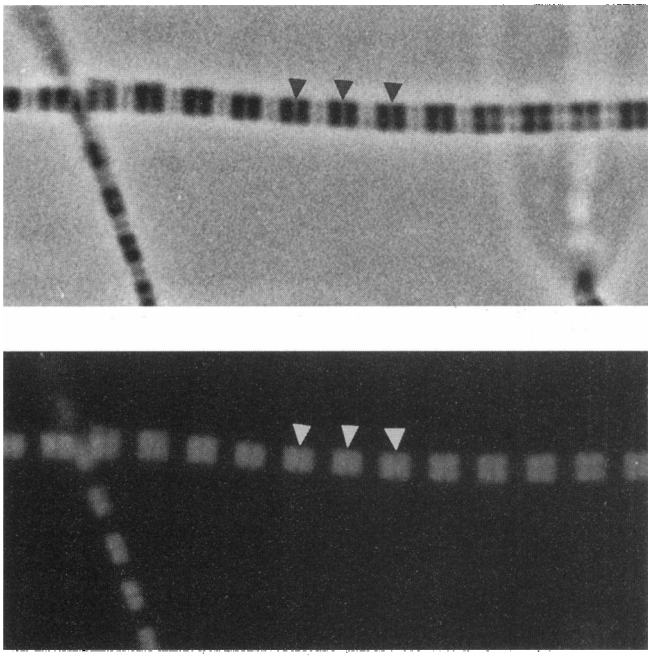

FIGURE 2 Phase contrast (*top*) and fluorescence (*bottom*) photomicrographs of myofibrils exchanged with cgRLC. Note the dark bands in the fluorescence image in the region of the M line (*arrows*).

target protein domain, and absence of modification of native structure or function by the probe or the method used to introduce it. How does the present approach measure up to these criteria?

In the experiments reported above the ATR probe is covalently attached to a single cysteine residue, at least in the case of the gizzard RLC, and the labeled RLC is incorporated specifically into the myosin heads (Fig. 2). However, a general problem with ATR probes has been the variability between different commercially available batches of iodo-ATR. In the course of the present work we discovered that different batches of iodo-ATR could give either a perpendicular or parallel orientation preference on RLC in rigor fibers. These differences are at least partly related to the presence of variable amounts of the 5- and 6-isomers of iodo-ATR. Pure iodo-ATR isomers have now been synthesized (Corrie and Craik, 1994) and used to label RLC (Sabido-David et al., 1994). The results show that the two batches of iodo-ATR used in the present work (9B or 10A from Molecular Probes) contained predominantly the 6-isomer.

Introduction of the ATR-cgRLC probe did alter the structure of relaxed, but not of rigor fibers, as judged by the low-angle x-ray diffraction patterns (Fig. 1). The axial and helical ordering of the myosin heads, characteristic of relaxed rabbit psoas muscle at 20°C, was largely lost after RLC exchange. This suggests that the normal packing of the heads on the surface of the thick filament has been disrupted, so that the structure may be more like that of relaxed muscle at low temperature (Wray, 1987). Consistent with this hypothesis, the polarization ratios from relaxed fibers showed no evidence of increased orientational order at higher temperatures. The loss of spatial order of the relaxed fibers at 20°C may be related to the use of gizzard RLC, the presence of the ATR probe, or some other effect of the exchange protocol. Whatever the detailed explanation, the orientational order may also have been affected by RLC exchange, so that the measured polarization ratios may not accurately represent the orientation distribution of native relaxed fibers at 20°C. There is no evidence for an effect of RLC exchange on the rigor structure (Fig. 1). The effect of RLC exchange on the x-ray pattern from contracting fibers is unknown.

Functional modification by RLC exchange seems relatively minor. Isometric force was only slightly reduced. The tension changes after photolysis of caged ATP in rigor fibers in the presence of Ca^{2+} (Allen et al., 1996) and the tension transients after rapid length steps in actively contracting fibers (Irving et al., 1995) are similar to those in control fibers. These results are broadly consistent with previous studies on functional effects of RLC removal and readdition (Moss et al., 1982; Moss, 1992; Lowey et al., 1993), showing that normal function was regained on adding back the native RLC. These studies suggest that exogenous RLC can rebind to the myosin heavy chain in a functional conformation.

The general conclusion of this section is that the present ATR-RLC approach gives a useful but non-ideal probe of the orientation of the light-chain region of the myosin head in muscle fibers. Qualitatively similar results were obtained with the native rabbit RLC and chicken gizzard RLC, but the latter has the advantage that the ATR probe is attached to a single cysteine residue. Other probe sites and RLC exchange protocols must be explored to improve preservation of the structure of relaxed fibers.

Quantitative interpretation of the polarization ratios

The polarization ratios reported above were interpreted in terms of probe orientation distributions using the formalism described in an accompanying paper (Irving, 1996). This allows the probes limited mobility on a time scale faster than the fluorescence lifetime, so that an individual probe may change its dipole orientation between absorbing and emitting a photon. The mobility was assumed to be confined to a cone of semi-angle δ, and wobble within the cone to be fast compared to the fluorescence lifetime. We also assumed that there is no fixed offset between the absorption and emission dipoles of rhodamine (Chen and Bowman, 1965). This assumption was supported by the present results: the polarization ratio for rhodamine immobilized in epoxy was 0.475, close to the expected value of 0.5 for parallel absorption and emission dipoles, and the fiber P and Q ratios, which depend predominantly on the orientation of the emission and absorption dipoles, respectively, were similar (Table 1).

Two simple models were used to describe the distribution of the orientations of the center axis of the cone with respect to the fiber axis. The first model assumes a fraction f of the cone axes are isotropically distributed and the remainder are at a fixed axial angle θ, as would result from a helical set of probes (Tregear and Mendelson, 1975). The second model assumes the axial distribution of cones is a gaussian function with peak angle θ_o and dispersion σ, i.e., the fraction of probes with axial angle θ is proportional to $\exp\{-(\beta - \theta_o)^2/2\sigma^2\}\sin\beta$, where polarized intensities were calculated by integrating over β between 0 and 180°. Thus in each model three parameters (δ, θ, and f in the helix plus isotropic model, and δ, θ_o, and σ in the gaussian model) are used to fit two observed polarization ratios, $P_\parallel$ and $P_\perp$. Fortunately δ can be obtained independently by varying the angle between the propagation axes of the exciting and fluorescent light, and is about 20° for the ATR-cgRLC probes in relaxed, rigor, and isometrically contracting muscle fibers (unpublished results of Hopkins, Shifman, Irving, and Goldman).

Table 5 shows the fits to the polarization ratios from ATR-labeled cgRLC in relaxation, rigor, and isometric contraction obtained with the helix plus isotropic and the gaussian models, and $\delta = 20°$. The fitted parameters for relaxation and isometric contraction are similar, as expected from

TABLE 5 Orientation distribution parameters for ATR-labeled cgRLC probes

	Helix plus isotropic		Gaussian	
	θ (degrees)	f (fraction isotropic)	θ_0 (degrees)	σ (degrees)
Relaxed	63.3	0.792	50.8	30.5
Contracting	61.8	0.788	50.9	28.7
Rigor	66.5	0.581	58.7	25.3
Rigor/S-1	68.1	0.576	60.3	28.5

Helix plus isotropic model: θ, orientation of the helically ordered fraction of probes with respect to the fiber axis; f, fraction of isotropically distributed probes. Gaussian model: θ_0, peak angle, and σ, dispersion, of the gaussian distribution of cone axes with respect to the fiber axis. In both cases δ, the semi-angle of the cone within which fluorophores diffuse freely on the time scale faster than the fluorescence lifetime, was set to 20°. Relaxed and rigor values from mean polarization ratios in Table 2; contracting values from Table 4.

the similarity between their respective P ratios. Likewise, the fitted parameters for rigor are close to those for exogenous myosin subfragment 1 (rigor/S-1).

In all conditions studied there was a high degree of orientational disorder. In the helix plus isotropic model the isotropic fraction (f) was greater than 0.5, and in the gaussian model the dispersion (σ) was greater than 25°. In the helix plus isotropic model, the isotropic fraction (f) was substantially smaller in rigor or rigor/S-1 than in relaxation or active contraction. However, the corresponding changes in dispersion (σ) in the gaussian model were relatively small, showing that conclusions about the degree of disorder based on a particular model for the orientation distribution should be treated with caution. The axial angle (θ) of the helical fraction of probes in the helix plus isotropic model was consistently larger than the peak angle of the gaussian distribution (θ_0). Both θ and θ_0 were higher in rigor or rigor/S-1 than in relaxation or active contraction, but the difference was larger for θ_0. Broadly similar conclusions about the orientation distributions of the ATR-cgRLC probes in relaxing and rigor conditions were derived from a separate set of measurements using a photoelastic modulator to measure the Q polarization ratios, which depend on the orientation of the absorption dipoles (Allen et al., 1996).

The parameters in Table 5 were obtained with the semi-angle of the wobble cone (δ) set to 20°, but are relatively insensitive to the value of δ in the range from 11°, the value that fits the isotropic polarization ratios for ATR immobilized in Araldite, to the values above which the orientation models failed to fit the fiber data for some experimental conditions. This upper limit was $\delta = 23°$ for the gaussian model and $\delta = 29°$ for the helix plus isotropic model. For example, in the case of the rigor polarization ratios in the helix plus isotropic model, $\delta = 11°$ gives $\theta = 64°, f = 0.53$; $\delta = 23°$ gives $\theta = 68°, f = 0.60$; $\delta = 29°$ gives $\theta = 74°$, $f = 0.65$. Similarly, in the gaussian model $\delta = 11°$ gives $\theta_0 = 58°$, $\sigma = 20°$, and $\delta = 23°$ gives $\theta_0 = 60°$, $\sigma = 30°$.

Orientation of the light-chain region of the myosin head in muscle fibers

Rigor

At short sarcomere length (2.4 μm) there was a marked preference for probe orientations perpendicular to the fiber axis. At sarcomere length 4.0 μm, where overlap between myosin- and actin-containing filaments should be abolished, the perpendicular orientation preference was much reduced and was similar to that of relaxed fibers at sarcomere length 4.0 μm. This suggests that the perpendicular orientation preference seen at the shorter sarcomere lengths is a consequence of myosin binding to actin in the absence of ATP. The perpendicular orientation preference observed with ATR-cgRLC exchanged into Mg-papain S-1 bound to actin filaments at sarcomere length 4.0 μm was approximately the same as that observed in the native myosin heads in rigor at short sarcomere length (2.4 μm). This also suggests that the perpendicular orientation preference is determined by actin binding rather than, for example, by an ATP-dependent interaction between the light-chain region of the myosin head and the thick filament. These results show that the orientation of the regulatory light-chain region of the myosin head depends on actin binding.

The ATR-cgRLC probe orientation distributions for rigor and exogenous S-1 (Table 5) have some similarities with those reported for electron paramagnetic resonance (EPR) probes on rabbit skeletal RLC (mainly on Cys 125) in rabbit psoas fibers (Hambly et al., 1991, 1992). These EPR spectra could be fitted by two populations of probes, one isotropic and immobile on the nanosecond time scale, and the other moving with a rotational correlation time of about 5 ns within a cone of half-angle 35° at about 74° to the fiber axis. In contrast, Arata (1990), using a different EPR probe probably attached to Cys 157 of rsRLC, found an isotropic distribution of probes in rigor fibers when the labeled RLC was exchanged into the native myosin heads, but a well-oriented population of probes with exogenous S-1. The divergent results may be related to the different probe sites or experimental protocols employed.

All of these studies found considerable orientational disorder of RLC probes in rigor. This might indicate disorder of the probes with respect to the light-chain region, as would be produced if the probes bound to the surface of the light-chain region with a broad range of conformations, even when tethered to a specific cysteine residue. In interpreting the polarization ratios we made the simplifying assumption (Irving, 1996) that probe motions are either very fast or very slow compared to the fluorescence lifetime (about 2 ns for ATR; Allen and Arner, 1995). The fast motions were described by subnanosecond wobble in a cone of semi-angle δ, and any slow motions would contribute to the disorder terms f and σ. In practice probe motions may occur on a time scale similar to the fluorescence lifetime and would then contribute to both the dynamic (δ) and static (f and σ) disorder terms in our interpretation.

Alternatively, the RLC probe disorder seen in rigor fibers and with S-1 decoration may reflect underlying orientational disorder of the light-chain region of the myosin heads. Some part of the myosin cross-bridge must be distorted to allow stereospecific binding at the actin-myosin interface in rigor, because the longitudinal periodicity of the actin binding sites does not match that of the myosin cross-bridge origins. A range of cross-bridge angles in rigor was observed in three-dimensional image reconstructions from electron micrographs of insect flight muscle (Taylor et al., 1989). The RLC probes also show substantial orientational disorder in exogenous myosin subfragment 1 bound to the actin filaments in fibers (Table 5), in the absence of any distortion due to the connection with the thick filaments. This may also reflect underlying disorder of the light-chain region of the myosin heads. In three-dimensional reconstructions from electron micrographs of actin filaments decorated with S-1 containing a full complement of light chains, this region has low density, indicating that it is disordered (Milligan and Flicker, 1987).

In contrast, probes on the Cys 707 of the myosin heavy chain, close to the nucleotide binding site, are well ordered in rigor for both native myosin heads and exogenous S-1 (Thomas and Cooke, 1980). Comparison with the present results suggests flexibility in the rigor head between the catalytic domain of the myosin head and the light-chain region. Stretching rigor fibers changes the orientation of the ATR-cgRLC probes (Irving et al., 1995), but not ATR probes on Cys 707 (Berger et al., 1994), which is consistent with this hypothesis.

Relaxation

The ATR-RLC probes were highly disordered in relaxed fibers. Previous studies with RLC EPR probes found an almost isotropic distribution of probe angles during relaxation (Arata, 1990; Hambly et al., 1991). The present results would be consistent with about 80% of the ATR-RLC probes being isotropically distributed in relaxed fibers (Table 5). Because the RLC exchange procedure resulted in substantial loss of the axial and helical order in the x-ray diffraction pattern from relaxed fibers (Fig. 1), some of the observed probe disorder may have been introduced by the RLC exchange. Furthermore, the orientation of the ATR-RLC probes was found to be insensitive to variation in temperature of relaxed fibers in the range 5–20°C, in contrast with the large changes in the x-ray diffraction pattern observed in these conditions (Wray, 1987; Lowy et al., 1991). The RLC exchange disrupts the helical tracks of myosin heads on the surface of the thick filament that are normally present at 20°C, and the resulting structure may be more like that of normal relaxed muscle at 5°C. Further experiments are required to characterize, and possibly reduce, the effects of RLC exchange on myosin head conformation in relaxed muscle.

Probes on Cys 707 and at the nucleotide binding site are also highly disordered in relaxed muscle (Thomas and Cooke, 1980; Crowder and Cooke, 1987; Reedy et al., 1992). Such disorder may be present under conditions in which x-ray diffraction and electron microscopy indicate the usual regular arrangement of myosin heads (Reedy et al., 1992). The dipole probes seem to be sensitive to types of disorder that are not readily resolved by x-ray diffraction or electron microscopy. Such types of disorder would include independent motion of small domains of the head, rotation of an elongated domain about its long axis (if the dipole axis were not parallel to the long axis), different conformations of the two heads of a myosin molecule, and the presence of a small population of actin-attached heads in relaxed muscle.

Isometric contraction

The polarization ratios from the ATR-RLC probes in isometrically contracting fibers were similar to those in relaxation, although there were small repeatable differences between the polarization ratios in the two conditions (Table 4). Small differences of the opposite sign were observed in comparing activation and relaxation produced by photolysis of caged ATP (Allen et al., 1996). The origin of these small differences is not clear. They might be related to differences in concentrations of ATP and its hydrolysis products in the fibers or to small changes in filament orientation, rather than to active contraction per se. Whatever the origin of these small changes, they have little effect on the fitted orientation distributions, which would be consistent with about 80% of the probes being isotropically distributed, as during relaxation (Table 5). EPR probes on RLC also show a high degree of orientational disorder during active contraction (Hambly et al., 1992).

It is not known whether the conformation of myosin heads in contracting muscle has been affected by RLC exchange, but isometric force and tension transients after photolysis of caged ATP (Allen et al., 1996) or rapid length steps (Irving et al., 1995) seem unaffected. Thus any structural changes produced by RLC exchange do not seem to have significant effects on the contractile mechanism.

During active contraction myosin heads perform ATPase cycles asynchronously, so all of the structural states in the cycle contribute to the orientation distribution observed in the present experiments. The multiplicity of states may be responsible for some of the observed orientational disorder. Other sources of probe disorder may also contribute, as discussed above for rigor and relaxing conditions. There was no evidence of the rigor-like orientation distribution appearing during isometric contraction, although a small fraction of probes with this orientation could not be excluded by the present results.

The ATR-RLC probes are not completely isotropic in contracting muscle, and the residual order allows the method to be used to follow structural changes in the light-chain region of the myosin heads associated with mechanical perturbations such as rapid length steps (Irving et al., 1995). Similarly, the characteristic differences in

polarization ratios between rigor and either relaxation or activation allow the kinetics of movements of the light-chain region after photolysis of caged ATP to be determined, as described in an accompanying paper (Allen et al., 1996).

We are grateful to Professor R. M. Simmons for his support in initiating this project, to Dr. M. A. Ferenczi and Mr. I. Dobbie for help with the x-ray experiments, to Dr. Y. E. Goldman for helpful comments on an earlier version of the manuscript, and to Mr. K. Eason and Mr. T. Rutherford for skilled technical assistance.

We are also grateful to the Muscular Dystrophy Association (USA), the Wellcome Trust (UK), the Medical Research Council (UK), and the Royal Society (UK) for financial support.

REFERENCES

Allen, T. St. C., and A. Arner. 1995. Time-resolved fluorescence spectroscopy of acetamidotetramethylrhodamine free in solution and bound to myosin regulatory light chain. *Biophys. J.* 68:A160.

Allen, T. St. C., N. Ling, M. Irving, and Y. E. Goldman. 1996. Orientation changes in myosin regulatory light chains following photorelease of ATP in skinned muscle fibers. *Biophys J.* 70:000–000.

Arata, T. 1990. Orientation of spin-labeled light chain-2 of myosin heads in muscle fibers. *J. Mol. Biol.* 214:471–478.

Berger, C. L., S. Karki, and Y. E. Goldman. 1994. Fluorescence polarization of acetamidotetramethylrhodamine (ATR) covalently bound to SH-1 in rabbit psoas muscle fibers following rapid length changes. *Biophys. J.* 66:A189.

Borejdo, J., O. Assulin, T. Ando, and S. Putnam. 1982. Cross-bridge orientation in skeletal muscle measured by linear dichroism of an extrinsic chromophore. *J. Mol. Biol.* 158:391–414.

Borejdo, J., S. Putnam, and M. F. Morales. 1979. Fluctuations in polarized fluorescence: evidence that muscle cross bridges rotate repetitively during contraction. *Proc. Natl. Acad. Sci. USA.* 76:6346–6350.

Burghardt, T. P., T. Ando, and J. Borejdo. 1983. Evidence for cross-bridge order in contraction of glycerinated skeletal muscle. *Proc. Nat. Acad. Sci. USA.* 80:7515–7519.

Chen, R. F., and R. L. Bowman. 1965. Fluorescence polarization: measurement with ultraviolet polarizing filters in a spectrophotofluorimeter. *Science.* 147:729–732.

Cooke, R. 1986. The mechanism of muscle contraction. *CRC Crit. Rev. Biochem.* 21:53–118.

Cooke, R., M. S. Crowder, and D. D. Thomas. 1982. Orientation of spin labels attached to cross-bridges in contracting muscle fibers. *Nature.* 300:776–778.

Corrie, J. E. T., and J. S. Craik. 1994. Synthesis and characterisation of pure isomers of iodoacetamidotetramethylrhodamine. *J. Chem. Soc. Perkins Trans.* 1:2967–2974.

Crowder, M. S., and R. Cooke. 1987. Orientation of spin-labeled nucleotides bound to myosin in glycerinated muscle fibers. *Biophys. J.* 51: 323–333.

Greaser, M. L., and J. Gergely. 1971. Reconstitution of troponin activity from three protein components. *J. Biol. Chem.* 246:4226–4233.

Hambly, B., K. Franks, and R. Cooke. 1991. Orientation of spin-labeled light chain-2 exchanged onto myosin cross-bridges in glycerinated muscle fibers. *Biophys. J.* 59:127–138.

Hambly, B., K. Franks, and R. Cooke. 1992. Paramagnetic spin probes attached to a light chain on the myosin head are highly disordered in active muscle fibers. *Biophys. J.* 63:1306–1313.

Huxley, A. F. 1957. Muscle structure and theories of contraction. *Prog. Biophys. Biophys. Chem.* 7:255–318.

Huxley, A. F., and R. M. Simmons. 1971. Proposed mechanism of force generation in striated muscle. *Nature.* 213:533–538.

Huxley, H. E. 1969. The mechanism of muscle contraction. *Science.* 164:1356–1366.

Irving, M. 1996. Steady state polarization from cylindrically symmetric fluorophores undergoing rapid restricted motion. *Biophys. J.* 70: 000–000.

Irving, M., T. St. C. Allen, C. Sabido-David, J. S. Craik, B. Brandmeier, J. Kendrick-Jones, J. E. T. Corrie, D. R. Trentham, and Y. E. Goldman. 1995. Tilting of the light chain region of myosin during step length changes and active force generation in skeletal muscle. *Nature.* 375: 688–691.

Irving, M., J. Kendrick-Jones, C. Shrimpton, and J. Sleep. 1989. The orientation of rhodamine probes attached to myosin light chain-2 (LC-2) in relaxing and rigor conditions in single fibers isolated from rabbit psoas muscle. *J. Physiol.* 418:57P.

Jakes, R., F. Northrop, and J. Kendrick-Jones. 1976. Calcium binding regions of myosin regulatory light chains. *FEBS Lett.* 70:229–234.

Katoh, T., and S. Lowey. 1989. Mapping myosin light chains by immunoelectron microscopy. Use of anti-fluorescyl antibodies as structural probes. *J. Cell Biol.* 109:1549–1560.

Kishino, A., and T. Yanagida. 1988. Force measurements by micromanipulation of a single actin filament by glass needles. *Nature.* 334:74–76.

Knight, P. J., and J. A. Trinick. 1982. Preparation of Myofibrils. *Methods Enzymol.* 85B:9–12.

Lowey, S., G. S. Waller, and K. M. Trybus. 1993. Skeletal muscle myosin light chains are essential for physiological speeds of shortening. *Nature.* 365:454–456.

Lowy, J., D. Popp, and A. A. Stewart. 1991. X-ray studies of order-disorder transitions in the myosin heads of skinned rabbit psoas muscles. *Biophys. J.* 60:812–824.

Lymn, R. W., and E. W. Taylor. 1971. Mechanism of adenosine triphosphate hydrolysis by actomyosin. *Biochemistry.* 10:4617–4624.

Margossian, S. S., and S. Lowey. 1982. Preparation of myosin and its subfragments from rabbit skeletal muscle. *Methods Enzymol.* 85:55–71.

Matsuda, G., T. Maita, Y. Suzuyama, M. Setoguchi, and T. Umegane. 1977. Amino acid sequence of the LC-2 light chain of rabbit skeletal muscle myosin. *J. Biochem. (Tokyo).* 81:809–811.

Milligan, R. A., and P. F. Flicker. 1987. Structural relationships of actin, myosin, and tropomyosin revealed by cryo-electron microscopy. *J. Cell Biol.* 105:29–39.

Moss, R. 1992. Ca^{2+} regulation of mechanical properties of striated muscle. *Circ. Res.* 70:865–883.

Moss, R. L., G. G. Giulian, and M. L. Greaser. 1982. Physiological effects accompanying the removal of myosin LC2 from skinned skeletal muscle fibers. *J. Biol. Chem.* 257:8588–8591.

Ostap, E. M., V. A. Barnett, and D. D. Thomas. 1995. Resolution of three structural states of spin-labeled myosin in contracting muscle. *Biophys. J.* 69:177–188.

Peckham, M., and M. Irving. 1989. Myosin crossbridge orientation in demembranated muscle fibers studied by birefringence and x-ray diffraction measurements. *J. Mol. Biol.* 210:113–126.

Penefsky, H. S. 1977. Reversible binding of Pi by beef heart mitochondrial adenosine triphosphatase. *J. Biol. Chem.* 252:2891–2899.

Rayment, I., H. M. Holden, M. Whittaker, C. B. Yohn, M. Lorenz, K. C. Holmes, and R. A. Milligan. 1993a. Structure of the actin-myosin complex and its implications for muscle contraction. *Science.* 261: 58–65.

Rayment, I., W. R. Rypniewski, K. Schmidt-Base, R. Smith, D. R. Tomchick, M. M. Benning, D. A. Winkelman, G. Wesenberg, and H. M. Holden. 1993b. Three dimensional structure of myosin subfragment-1: a molecular motor. *Science.* 261:50–58.

Reedy, M. K., K. C. Holmes, and R. T. Tregear. 1965. Induced changes in orientation of the cross-bridges of glycerinated insect flight muscle. *Nature.* 207:1276–1280.

Reedy, M. K., N. Lucaveche, N. Naber, and R. Cooke. 1992. Insect crossbridges, relaxed by spin labeled nucleotide, show well-ordered 90° state by x-ray diffraction and electron microscopy, but spectra of electron paramagnetic resonance probes report disorder. *J. Mol. Biol.* 227: 678–697.

Rowe, T., and J. Kendrick-Jones. 1992. Chimeric myosin regulatory light chains identify the subdomain responsible for regulatory function. *EMBO J.* 11:4715–4722.

Sabido-David, C., J. S. Craik, B. Brandmeier, J. E. T. Corrie, D. R. Trentham, N. Ling, and M. Irving. 1994. Orientation of acetamidotetramethylrhodamine (ATR) isomers covalently bound to regulatory light chains in rabbit psoas muscle fibers. *Biophys. J.* 66:A234.

Sleep, J. 1990. Temperature control and exchange of the bathing solution for skinned muscle fibers. *J. Physiol.* 423:7P.

Tanner, J. W., D. D. Thomas, and Y. E. Goldman. 1992. Transients in orientation of a fluorescent cross-bridge probe following photolysis of caged nucleotides in skeletal muscle fibers. *J. Mol. Biol.* 223:185–203.

Taylor, K. A., M. C. Reedy, L. Córdova, and M. K. Reedy. 1989. Three dimensional image reconstruction of insect flight muscle. II. The rigor actin layer. *J. Cell Biol.* 109:1103–1123.

Thomas, D. D. 1987. Spectroscopic probes of muscle crossbridge rotation. *Annu. Rev. Physiol.* 49:691–709

Thomas, D. D., and R. Cooke. 1980. Orientation of spin-labeled myosin heads in glycerinated muscle fibers. *Biophys. J.* 32:891–906.

Towns-Andrews, E., A. Berry, J. Bordas, G. R. Mant, P. K. Murray, K. Roberts, I. Sumner, J. S. Worgan, R. Lewis, and A. Gabriel. 1989. Time-resolved x-ray diffraction station: x-ray optics, detectors, and data acquisition. *Rev. Sci. Instrum.* 60:2346–2349.

Tregear, R. T., and R. M. Mendelson. 1975. Polarization from a helix of fluorophores and its relation to that obtained from muscle. *Biophys. J.* 15:455–467.

Vibert, P., and C. Cohen. 1988. Domains, motions and regulation in the myosin head. *J. Muscle Res. Cell Motil.* 9:296–305.

Wagner, P. D. 1982. Preparation and fractionation of myosin light chains and exchange of the essential light chains. *Methods Enzymol.* 85:72–81.

Wray, J. S. 1987. Structure of relaxed myosin filaments in relation to nucleotide state in vertebrate skeletal muscle. *J. Muscle Res. Cell Motil.* 8:62a.

Yanagida, T. 1981. Angles of nucleotides bound to cross-bridges in glycerinated muscle fiber at various concentrations of ϵ-ATP, ϵ-ADP and ϵ-AMP. PNP detected by polarized fluorescence. *J. Mol. Biol.* 146:539–560.